J. Phycol. **55,** 1028–1040 (2019)

DOI: 10.1111/jpy.12865

MIXOTROPHIC TRADE-OFF UNDER WARMING AND UVR IN A MARINE AND A FRESHWATER ALGA[1]

Juan Manuel González-Olalla[2], *Juan Manuel Medina-Sánchez*, *and Presentación Carrillo*

University Institute of Water Research, University of Granada, C/Ramón y Cajal, 4, Granada 18071, Spain
Department of Ecology, Faculty of Sciences, University of Granada, Campus Fuentenueva s/n, Granada 18071, Spain
jmolalla@ugr.es

Mixotrophic protists combine phagotrophy and phototrophy within a single cell. Greater phagotrophic activity could reinforce the bypass of carbon (C) flux through the bacteria-mixotroph link and thus lead to a more efficient transfer of C and other nutrients to the top of the trophic web. Determining how foreseeable changes in temperature and UVR affect mixotrophic trade-offs in favor of one or the other nutritional strategy, along the mixotrophic gradient, is key to understanding the fate of carbon and mineral nutrients in the aquatic ecosystem. Our two main hypotheses were: (i) that increased warming and UVR will divert metabolism toward phagotrophy, and (ii) that the magnitude of this shift will vary according to the organism's position along the mixotrophic gradient. To test these hypotheses, we used two protists (*Isochrysis galbana* and *Chromulina* sp.) located in different positions on the mixotrophic gradient, subjecting them to the action of temperature and of UVR and their interaction. Our results showed that the joint action of these two factors increased the primary production: bacterivory ratio and stoichiometric values (N:P ratio) close to Redfield's ratio. Therefore, temperature and UVR shifted the metabolism of both organisms toward greater phototrophy regardless of the original position of the organism on the mixotrophic gradient. Weaker phagotrophic activity could cause a less efficient transfer of C to the top of trophic webs.

***Key index words: Chromulina*; elemental composition; interactive effects; *Isochrysis*; mixotrophic phytoplankton; phagotrophy; photosynthesis; UVR; warming**

***Abbreviations*: BV, bacterivory; EOC, excreted organic carbon; NPQ, nonphotochemical quenching; PP, primary production; R, respiration; Φ_{PSII}, photosynthetic quantum yield**

Mixotrophy, a metabolic trait long considered an exception, today is known to include most aquatic protists. This type of metabolism combines the acquisition of C or mineral nutrients through more than one trophic mode (Selosse et al. 2017). Mixotrophs are capable not only of photosynthesis but also of bacterial predation through phagotrophy. This dual ability is shared by most phylogenetic branches, clades, such as chrysophytes and haptophytes (Chan et al. 2018). All of these protists are widespread in natural communities (Unrein et al. 2007, Zubkov and Tarran 2008), especially in oligotrophic waters (Modenutti 2014), presumably due to their trophic advantage of acquiring limiting nutrients through bacterial predation (Raven et al. 2009, Tsai et al. 2016). From this perspective, the former paradigm of two protist groups (i.e., photoautotrophs and phagoheterotrophs) now includes mixotrophs as a new functional classification (Mitra et al. 2016).

Different numerical and experimental studies have demonstrated that mixotrophs exert a strong impact on aquatic ecosystems, boosting primary production and bacterial production, transferring C biomass to higher trophic levels, and stimulating the C-flux sink (e.g., Mitra et al. 2014, Ward and Follows 2016). With the inclusion of mixotrophs into trophic-web models, the prediction of how mixo-phytoplankton communities will respond to multiple environmental changes is currently a major scientific challenge (Reusch and Boyd 2013, Cabrerizo et al. 2018). This requires quantifying how mixotrophic species with different positions in the gradient between photoautotrophy and heterotrophy respond to multiple stressors (Flynn et al. 2013).

A complex stressor, the climate change-associated temperature rise (IPCC 2013), accentuates the stratification and shallowing of upper mixing layer in aquatic ecosystems. This stratification traps the organisms in surface waters, exposing them to intense radiation with high ultraviolet levels (UVR, 280–400 nm; Villafañe et al. 2003, Carrillo et al. 2015). Also, the temperature increase reportedly affects phytoplankton, from raising the maximum quantum yield of photosystem II (PSII; Takahashi et al. 2013) to stunting growth (Halac et al. 2013, Cabrerizo et al. 2014). In addition, temperature can alter protist morphology (Mühling et al. 2003,

[1]Received 22 December 2018. Accepted 15 March 2019. First Published Online 18 April 2019. Published Online 25 May 2019, Wiley Online Library (wileyonlinelibrary.com).
[2]Author for correspondence: e-mail jmolalla@ugr.es.
Editorial Responsibility: T. Mock (Associate Editor)

Takabayashi et al. 2006), chlorophyll content (Verity 1981) and the C:N:P composition (Yvon-Durocher et al. 2015). These latter authors have demonstrated that a higher sea-surface temperature is significantly and directly related to N:P and C:P ratios of marine algal assemblages, mainly because of the decline in P-rich ribosomes. Moreover, warming over an entire range from 13°C to 33°C (Wilken et al. 2012) and an increase of 5°C (Cabrerizo et al. 2018) exerts a stronger positive effect on phagotrophy than on phototrophy, although a temperature rise of 4°C can also aid both processes (Princiotta et al. 2016).

The shallowing of the upper mixing layer implies more intense UVR exposure for phytoplankton, which damages different cell components (i.e., DNA) and/or depresses photosynthesis and growth (Buma et al. 2003, Villafañe et al. 2003). However, in high-mountain lakes, mixotrophs have been shown to outcompete strict autotrophs under high UVR intensities (Carrillo et al. 2017), presumably because mixotrophs can tolerate the inhibition of C fixation or PSII, by taking up C through bacterivory (BV; Medina-Sánchez et al. 2004). Furthermore, it has been shown that UVR directly influences the elemental composition of phytoplankton by decreasing the sestonic C:P and N:P ratios (Rojo et al. 2012, Carrillo et al. 2015).

Today, it is increasingly evident that synergistic and antagonistic interactions among drivers must be taken into account in order to provide more realistic predictions of future ecosystem changes (Jackson et al. 2016, Villar-Argaiz et al. 2018). Several short-term experiments have indicated that a rise in temperature promotes photochemical activity, improving the response to PAR and/or UVR (Sobrino and Neale 2007, Halac et al. 2010, Villafañe et al. 2013). Likewise, temperature and UVR may alter metabolic activity of strict photoautotrophic protists, including shifts in their elemental composition, and altering the transfer of C and other limiting nutrients to higher trophic levels (Joint and Jordan 2008, Montagnes et al. 2008). In addition, in a long-term experiment, the simultaneous action of warming and UVR has been found to reinforce the phagotrophic metabolism of *Isochrysis galbana* (Cabrerizo et al. 2018). However, in the current global warming scenario (see above), temperature could be understood as a press disturbance (i.e., chronic stress), whereas the UV radiation exposure would rather reflect a pulse disturbance (i.e., a combination of great intensity and short duration; see Harris et al. 2018). Therefore, it is key to evaluate the mixotrophic response to factors acting sequentially (Press vs. Pulse) on species and to quantify whether the magnitude of such a response depends on the organism's position in the mixotrophic gradient. Moreover, the stoichiometry modulating these responses might have a stronger explanatory role than previously thought.

We hypothesized: (i) that warming, UVR, and/or their interaction will shift the metabolism of mixotrophic protists toward greater phagotrophy; and (ii) that the magnitude of this shift will vary according to the organism's position along the mixotrophic gradient. Our hypotheses were tested with monospecific cultures of two characteristic species from marine and freshwater, and an a priori different position in the mixotrophic gradient. That is, *Isochrysis galbana* (Prymnesiophyceae) usually behaves proportionally more as a phototroph than a phagotroph (Anderson et al. 2018, Cabrerizo et al. 2018), whereas *Chromulina* sp. (Chrysophyceae) shows great versatility in its nutritional mode (Rottberger et al. 2013), although it usually acts as a phagotroph (Jones and Ilmavirta 1988).

MATERIAL AND METHODS

Species and culture mediums. *Isochrysis galbana* (Playa Unión, Argentina) was grown in F/2 medium (Guillard and Ryther 1962), and *Chromulina* sp. (CCAC, Culture collection of Algae at the University of Cologne, Germany) was grown in SFM medium (Synthetic Freshwater Medium; CCAC, Germany) at 19°C.

Experimental set-up. The experiment was a split-plot design to study the effect on mixotrophic trade-off of a press (temperature) and a pulse factor (UVR), both being global-change drivers (see Introduction). The design included two temperature treatments (19°C and 22°C) applied at the plot level and four temperature × light treatments (19_{-UVR}, 19_{+UVR}, 22_{-UVR}, 22_{+UVR}) at the subplot level stemming from the combination of (i) two temperature levels, low and high temperature (19°C and 22°C, respectively) and (ii) two light levels, +UVR (>280 nm) versus -UVR (only photosynthetically active radiation, PAR; >400 nm; Fig. 1). The increase of 3°C of temperature is within the variation expected in global predictions for the late 21st century (IPCC 2013, Scenario RCP8.5).

In the first part of the experiment (main plot, Fig. 1), both cultures were maintained in exponential growth for at least 11 generations (30 d) prior to any measurement. The cultures grew under a 12:12 h light:dark photoperiod, at the respective experimental temperature (19°C and 22°C) in 3 L flasks (one flask per species and temperature level). Both species were grown under mixotrophic conditions (nonaxenic culture) at 21.7 $W \cdot m^{-2}$ (~100 μmol photons $\cdot m^{-2} \cdot s^{-1}$) of PAR (400–700 nm). Bacteria growing in each culture were those naturally associated with protist species culture (bacteria were not identified).

In the second part of the experiment (subplot, Fig. 1), aliquots from the cultures were transferred to 12 quartz flasks (250 mL, $n = 3$ per treatment) for each species. The flasks were placed in an aquarium system with adjustable temperature by refrigeration (Teco® S. R. L. tank TK 2000, EU) and radiation through light-emitting diode lamps (nano

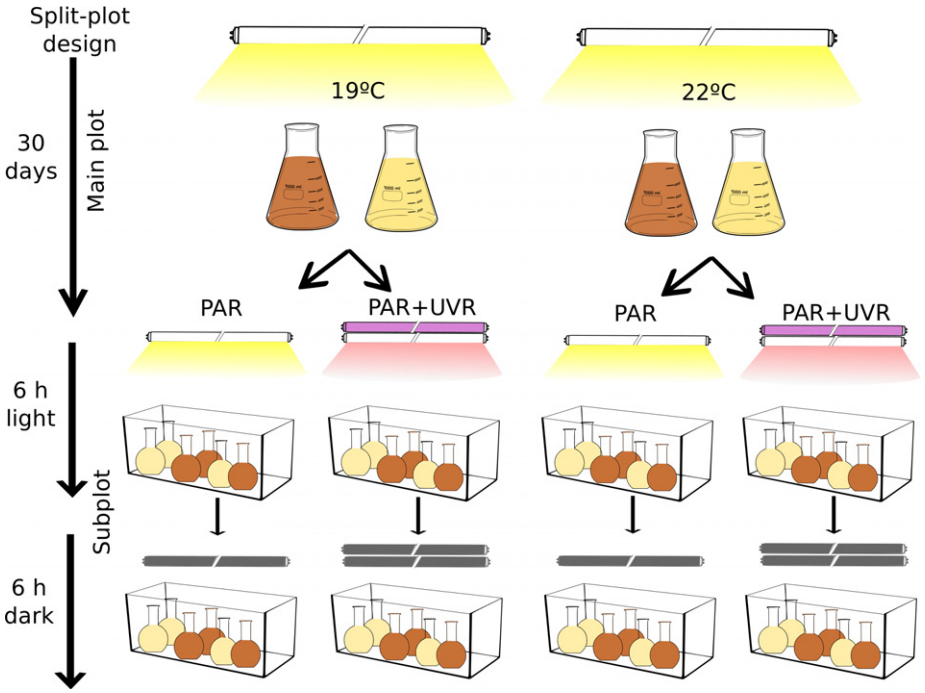

FIG. 1. Graphic scheme of the experimental split-plot design for each species (*Isochrysis galbana* and *Chromulina* sp.).The design included two temperature (T) treatments (19°C and 22°C) applied at the main plot level and four T × light treatments at the subplot level (19_{-UVR}, 19_{+UVR}, 22_{-UVR}, 22_{+UVR}). [Color figure can be viewed at wileyonlinelibrary.com]

LED light v.2.0, BLAU aquaristic) for PAR, and Q-Panel tubes for UVR (Fig. 1). For 12 h, the cultures were subjected to a photoperiod of 6:6 h light:dark, with irradiance of 21.7 $W \cdot m^{-2}$ (100 µmol photons $\cdot m^2 \cdot s^{-1}$) of PAR and an additional 2.42 $W \cdot m^{-2}$ of UVR in the +UVR treatments.

From flasks, aliquots were taken to measure photosynthetic quantum yield (Φ_{PSII}), cell-specific Chl *a*, elemental C, N, and P (see below). Furthermore, 40-mL Teflon FEP narrow-mouth bottles (Nalgene) were filled in triplicate to measure respiration (R), PP, and BV.

Response variables. The response variables measured were the most relevant ones for stoichiometry as well as phototropic and phagotrophic metabolism of mixotrophs (see Introduction).

Stoichiometric variables: Elemental composition (C, N, and P) of each algal species was determined from 15 mL of each experimental unit by low-pressure filtration (<100 mmHg) through precombusted (1 h at 550°C) glass-fiber filters of 1 µm pore size (Whatman GF/B; Whatman®, Sanford, ME, USA). Filters (one for C and N determination and another for P) were immediately frozen at −20°C. The C and N analyses were performed using a Perkin-Elmer 2400 elemental analyzer. Elemental P was determined after the filters were digested with a mixture of potassium persulfate and boric acid at 120°C for 30 min and analyzed as soluble reactive P by applying the acid molybdate technique (APHA 1992).

Chlorophyll a concentration: For the Chl *a* determination, 15 mL from each experimental unit was filtered through a Whatman GF/F filter (0.7 µm pore size), and the photosynthetic pigments were extracted during 24 h in darkness in 5 mL of acetone at 4°C to remove all the chlorophyll from the filters. The samples were measured at an excitation wavelength of 460 nm and emission at 670 nm, with a fluorometer LS 55 Luminescence Spectrometer (Perkin-Elmer, Boston, MA, USA). Previously, a calibration curve was made with pure spinach chlorophyll extract to transform fluorescence values into chlorophyll concentration.

Photosynthetic activity: *Chlorophyll fluorescence* — An amount of 3 mL from each experimental unit was taken every 2 h throughout the experiment to measure in vivo the Chl *a* fluorescence using a portable pulse-amplitude-modulated fluorometer (Water-ED PAM, Walz, Germany). Because the time between sampling and fluorescence measurements was a few seconds, the intrinsic photochemical efficiency of PSII (Φ_{PSII}) in the light was determined (Maxwell and Johnson 2000) as equation 1:

$$\Phi_{PSII} = \Delta F/(F'_m) = (F'_m - F'_t)/(F'_m) \quad (1)$$

where F'_m is the instantaneous maximum fluorescence induced by a saturating light pulse (ca. 5,300 µmol photons $\cdot m^{-2} \cdot s^{-1}$ in 0.8 s), and F_t is the current steady-state fluorescence induced by an

actinic light ~100 μmol photons · m^{-2} · s^{-1} in light-adapted cells. Each subsample was measured six times immediately after sampling, with each measurement lasting 10 s.

Nonphotochemical quenching: Nonphotochemical quenching (NPQ) was used as a proxy of the dissipation of the excess energy as heat and was determined directly from the PAM fluorometer as equation 2:

$$\mathrm{NPQ} = (F_m - F'_m)/(F'_m) \quad (2)$$

where F_m is the maximal fluorescence of dark-adapted sample and F'_m is the instantaneous maximum fluorescence induced by a saturating light pulse (c. 5,300 μmol photons · m^{-2} · s^{-1} in 0.8 s). This is the most important short-term photoprotective mechanism activated by saturating radiation intensities. The software stored the Fm value that was then used with each sample to calculate the NPQ.

The Φ_{PSII} and NPQ areas were calculated for Φ_{PSII} and NPQ diel cycles (in triplicate for each treatment), following González-Olalla et al. (2017), as in equation 3:

$$A = \int_b^a f(x)\,dx \quad (3)$$

where a and b are the initial and final measurement times, respectively, and $f(x)$ is the curve describing the yield or NPQ over time for each treatment. The area under the curve was calculated using the software MATLAB® r2015a (Mathworks, Natick, MA, USA).

Primary production: Following the ^{14}C method proposed by Nielsen (1952) and modified by Carrillo et al. (2002), 40-mL Teflon flasks were filled from each experimental unit (three clear plus one dark as control) and added with 9.25 MBq of $NaH^{14}CO_3$ (specific activity: 310.8 MBq · $mmol^{-1}$; DHI Water and Environment, Germany). The flasks were incubated for 2 h during the central hours of light exposure, and then fixed with neutralized formaldehyde 0.5% w/v final concentration and stored at 4°C until processed. Then, 40-mL aliquots were filtered through Nuclepore filters of 1-μm pore size to determine the particulate PP. The filtrations were gently carried out at low pressure (<100 mmHg) to minimize cell breakage. The excreted organic carbon (EOC) was measured from 4-mL aliquots of the filtrate (<1 μm). The filters and filtrate were put into 5- and 20-mL scintillation vials, respectively, and acidified with 100 μL of 1 N HCl to remove $DI^{14}C$. Vials were then kept open for 24 h in an aeration hood following the recommendations of Lignell (1992). Then, the vials were filled with scintillation cocktail (Ecoscint A) and counted using a scintillation counter (Beckman LS 6000TA) equipped with autocalibration. Total Organic Carbon (TOC) was calculated as sum of PP and EOC, and the %EOC was calculated following the equation 4:

$$\%\mathrm{EOC} = \frac{\mathrm{EOC}}{\mathrm{TOC}} \times 100 \quad (4)$$

Bacterivory rate: The method of Medina-Sánchez et al. (2004) was used to measure the amount of growing bacteria traced with [methyl-^{3}H]-thymidine captured by mixotrophic protists. For determining BV, aliquots of 15 mL from each experimental unit were transferred to 40-mL Teflon flasks, added with [Methyl ^{3}H]-thymidine to a final concentration of 25 nM, and incubated during 1 h at each corresponding temperature × light treatment (three replicates and one blank per treatment). After incubation, the BV was stopped by adding neutralized formaldehyde (0.75% w/v final concentration). Likewise, blanks were formaldehyde-killed before the incubation. The samples were preserved at 4°C until processed in the laboratory. A volume of 1.5 mL was taken from each replicate for determining the total activity (i.e., total traced bacteria) in the sample. The remaining sample volume (13.5 mL) was filtered through a cellulose nitrate filter of 1.2 μm pore size (Sartorius). A volume of 1.5 mL was taken from the filtrate to determine the residual activity (i.e., traced bacteria not captured by protists), while the activity registered on the filter (i.e., traced bacteria captured by protists) served to measure the BV. The filters were dissolved using 100% acetone and centrifuged at 16,000*g* for 10 min at 4°C. Supernatant acetone was eliminated without removing the pellet, which was finally fixed and re-suspended with 1.5 mL of TCA (5% final concentration). After TCA extraction (>20 min at <1°C), the precipitate was collected by centrifugation at 16,000 *g* for 10 min at 4°C, rinsed and centrifuged twice with 5% TCA, and measured in a scintillation counter equipped with autocalibration (Beckman LS 6000 TA). The conversion factor 1.5×10^{18} cells · mol^{-1} was used to convert the incorporated ^{3}H-thymidine into the number of depredated bacteria (Bell et al. 1983). The factor 20 fg C · $cell^{-1}$ was applied to convert depredated bacteria into C units (Lee and Fuhrman 1987).

Respiration rate: From each experimental unit, 40-mL Teflon flasks equipped with sensor spots (SP-PSt3-NAU-D5-YOP), were filled without bubbles, sealed to avoid gas exchanges, and incubated at each experimental temperature for 6 h in dark after the corresponding light-exposure period (three replicates per treatment). Measurements were made continuously using an oxygen transmitter (OXY-4 mini, Presens GmbH, Germany) equipped with Oxyview 6.02 software to register the data. This system was previously calibrated using two-point calibration (0% and 100% oxygen saturation) controlling temperature and atmospheric-pressure measurements. Respiration rates (in μg C · mg C^{-1} · h^{-1}) were calculated as the

slope of the regression fit of oxygen concentrations per C unit versus time. Oxygen values were converted to C units assuming a respiratory quotient of 1 (Del Giorgio and Cole 1998).

Effect size and statistical analysis. The statistical significance of temperature as the main plot effect, and temperature × UVR interaction as the subplot effect, on each response variable (see above) was assessed by two-way split plot of repeated-measures analysis of variance (RM-ANOVA) after verifying the assumptions of homoscedasticity for each data group (using Levene's tests) and normality of residuals (by Shapiro–Wilk's test).

The effect size of temperature, UVR, and temperature × UVR interaction, as a measurement of the magnitude and direction of factor effect on the response variables (cell-specific Chl *a*, C-, N-, P cell quota, C:N and C:P ratio, specific-PP, Φ_{PSII} area, specific-BV, R, %EOC, and NPQ area) for each species was calculated as follows in equations 5–7:

$$\text{Effect size of temperature}(\%) = \frac{X_{19-\text{UVR}} - X_{22-\text{UVR}}}{X_{19-\text{UVR}}} \times 100 \quad (5)$$

$$\text{Effect size of UVR}(\%) = \frac{X_{19-\text{UVR}} - X_{19+\text{UVR}}}{X_{19-\text{UVR}}} \times 100 \quad (6)$$

$$\text{Effect size of temperature} \times \text{UVR}(\%) = \frac{X_{19-\text{UVR}} - X_{22+\text{UVR}}}{X_{19-\text{UVR}}} \times 100 \quad (7)$$

where X is the response variable measured in the samples. Negative values indicate a stimulatory effect and positive values indicate an inhibitory effect of stress factors. Error propagation was used to calculate the variance of the effect size (as a percentage).

The differences between species for each response variable, (i) under identical experimental conditions and (ii) for the effect size of temperature, UVR, and temperature × UVR, were assessed by a *t*-test for independent samples after verifying the assumption of homoscedasticity (using Levene's test). All analyses were performed with the STATISTICA v7.0 software (Statsoft Inc. 2005).

RESULTS

Chl a *and stoichiometric responses.* Overall, the cell-specific Chl *a*, C-, N-, and P cell quota values were lower in *Isochrysis galbana* than in *Chromulina* sp. (*t*-test $P < 0.05$; Table S1 in the Supporting Information, Fig. 2, a–d). The C:N was higher and N:P lower than respective Redfield's ratios in *I. galbana*, whereas an opposite pattern was found in *Chromulina* sp. (except for the 19_{+UVR} treatment; Fig. 2, e and f). temperature × UVR interaction was significant for all these variables, except for the C cell quota and N:P ratio in *I. galbana* (Subplot effect; Table S2 in the Supporting Information).

The effect size of temperature, UVR, and temperature × UVR on cell-specific Chl *a* was weak (<15%), being that of temperature and temperature × UVR stimulatory in *Isochrysis galbana* but inhibitory in *Chromulina* sp. However, the effect size of UVR had an opposite pattern on both species ($P < 0.05$; Table S3 in the Supporting Information; Fig. 3a). Regarding elemental stoichiometric variables, the effect size of all factors was stimulatory in *I. galbana* (except those of temperature × UVR on C cell quota [no effect] and temperature on the N cell quota [inhibitory]), but inhibitory in *Chromulina* sp. (except that of temperature on the N cell quota [no effect]; $P < 0.05$, Table S3; Fig. 3, b–d). The effect size of UVR and temperature × UVR on the N cell quota was found to be greater in both species (exceeding 50%, Fig. 3c). For C:P and N:P ratios, only the effect size of temperature in *I. galbana* and, notably, the effect size of UVR in *Chromulina* sp., proved stimulatory on C:N ratio, whereas the effect size of UVR and temperature × UVR was stimulatory on N:P ratio only in *I. galbana* (Fig. 3, e and f).

Mixotrophic metabolism response to temperature and UVR. Isochrysis galbana and *Chromulina* sp. showed contrasting responses in the values of metabolic rates and in the magnitude and direction of the effect size of temperature, UVR, and temperature × UVR on most of these variables. Thus, the Φ_{PSII} area was higher in *I. galbana* than in *Chromulina* sp. (*t*-test $P < 0.05$; Table S1; Fig. 4a), whereas NPQ was lower in *I. galbana* than in *Chromulina* sp. (*t*-test $P < 0.05$; Table S1; Fig. S1a in the Supporting Information). The specific-PP values in *I. galbana* were ca. 1/5 of those in *Chromulina* sp. ($P < 0.05$; Table S1; Fig. 4b). Accordingly, the % EOC values range 53.8%–72.2%, were higher in *I. galbana* than in *Chromulina* sp. ($P < 0.05$; Table S1; Fig. S1b). temperature × UVR interaction was significant for all these variables, but opposite effects between species were found (subplot effect; Table S4 in the Supporting Information). The effect size of temperature and temperature × UVR on Φ_{PSII} area was inhibitory in *I. galbana* but stimulatory in *Chromulina* sp. ($P < 0.05$; Table S3; Fig. 5a), while the effect size of UVR was inhibitory in both species, with higher magnitude in *I. galbana* than in *Chromulina* sp. ($P < 0.05$; Table S3; Fig. 5a). Accordingly, the effect size of temperature, UVR, and temperature × UVR on NPQ was stimulatory (even exceeding 100%), in *I. galbana* but inhibitory in *Chromulina* sp. ($P < 0.05$; Table S3; Fig. 5c). In contrast to Φ_{PSII} area, the effect size of temperature, UVR, and temperature × UVR was stimulatory on specific-PP in *I. galbana*, but inhibitory in *Chromulina* sp. (except for UVR; Fig. 5b). Notably, the effect size of temperature, UVR, and temperature × UVR on %EOC was inhibitory in both *I. galbana* and

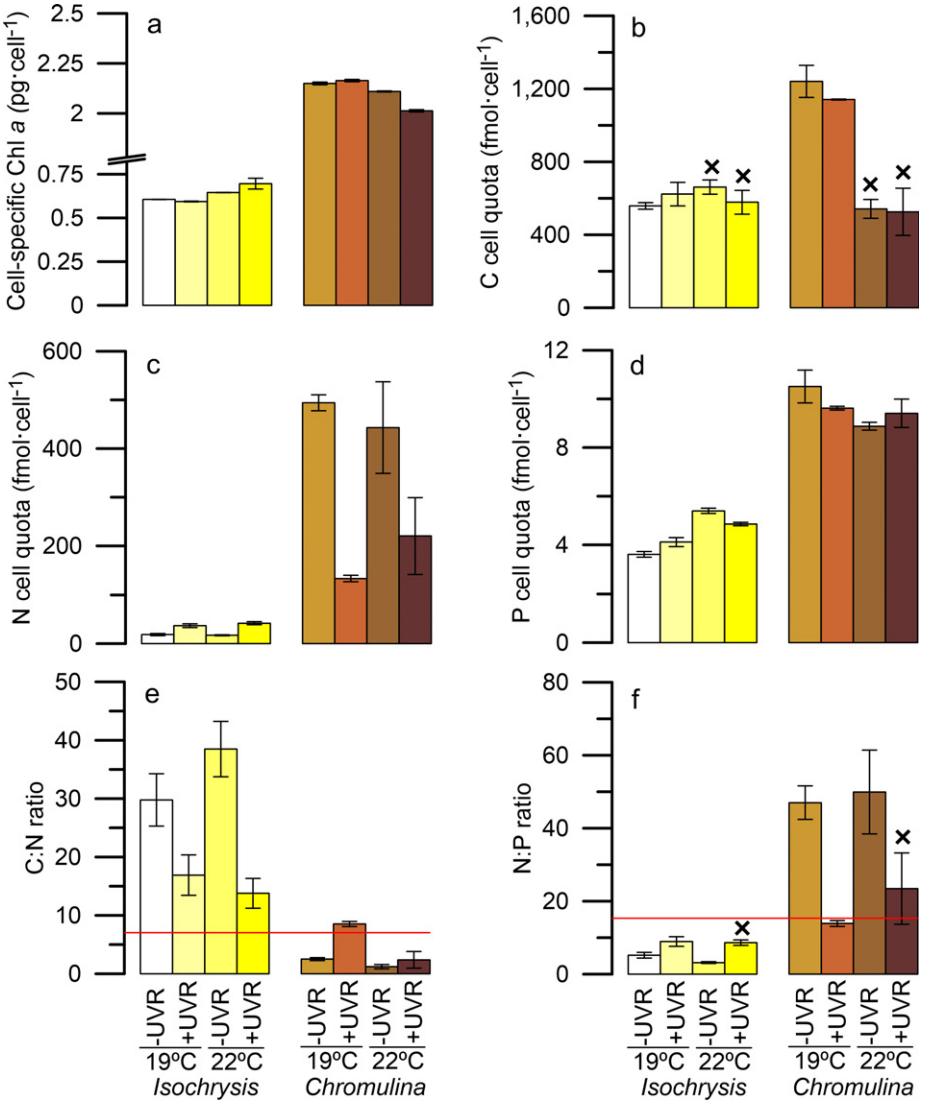

FIG. 2. Chlorophyll *a* content and elemental composition of *Isochrysis galbana* and *Chromulina* sp. under temperature (T) (low T [19°C] and high T [22°C]) and light (full sunlight [+UVR] and photosynthetically active radiation [−UVR]) treatments. Cell-specific Chl *a* (a), C cell quota (b), N cell quota (c) and P cell quota (d), C:N ratio (e) and N:P ratio (f). Red line represents Redfield ratio. Cross symbols represent the experimental conditions that did not exhibit significant differences between species. Data are expressed as mean values ± SD (n = 3). [Color figure can be viewed at wileyonlinelibrary.com]

Chromulina sp., although their magnitudes were lower in *I. galbana* ($P < 0.05$ for UVR and temperature × UVR; Table S3; Fig. 5d).

Regarding heterotrophic metabolism, the specific-BV was significantly higher in *Isochrysis galbana* than in *Chromulina* sp. (*t*-test $P < 0.05$; Table S1; Fig. 4c). The %BV in *I. galbana* and *Chromulina* sp. ranged from 1% to 35%, suggesting that mixotrophic protist activity was not limited by prey. Likewise, R rate was higher in *I. galbana* than in *Chromulina* sp. ($P < 0.05$; Table S1; Fig. S1c). There were significant temperature × UVR effects on both specific-BV and R rate in both species (subplot effect; Table S4). For specific-BV, the effect size of temperature was stimulatory, although the magnitude was lower in *Isochrysis galbana* (140%) than in *Chromulina* sp. (>700%). The effect size of UVR was opposite in the two species, being moderately (50%) inhibitory in *I. galbana* but strongly (>200%) stimulatory in *Chromulina* sp. ($P < 0.05$; Table S3; Fig. 5e). Finally, the effect size of temperature × UVR was (≈50%) inhibitory in both species, without significant differences between them ($P > 0.05$; Table S3; Fig. 5e). For R rate, the effect size of temperature and temperature × UVR was stimulatory for both species (Fig. 5f), the magnitude being greater in *Chromulina* sp. than in *I. galbana*, whereas the effect size of UVR was inhibitory in *I. galbana* but stimulatory in *Chromulina* sp. ($P < 0.05$; Table S3; Fig. 5f).

The PP:BV ratio was about two orders of magnitude higher in *Chromulina* sp. than in

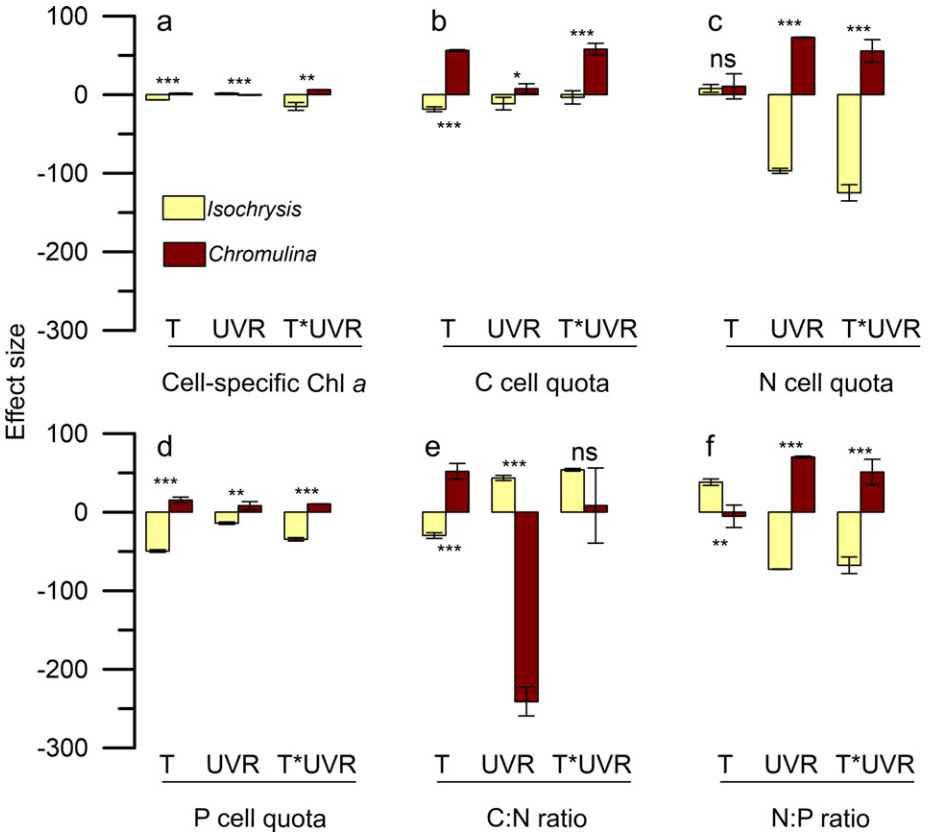

FIG. 3. Effect size of temperature (T), UVR, and temperature (T) × UVR on cell-specific Chl *a* (a), C cell quota (b), N cell quota (c) and P cell quota (d), C:N ratio (e) and N:P ratio (f) of *Isochrysis galbana* and *Chromulina* sp. Data are expressed as mean values ± SD ($n = 3$). Asterisks show the significance value: ***$P < 0.001$; **$P < 0.01$; *$P < 0.05$; ns: not significant. [Color figure can be viewed at wileyonlinelibrary.com]

Isochrysis galbana ($P < 0.05$; Table S1; Fig. 4d). The effect size of temperature was inhibitory in both species, although of magnitude proved lower in *I. galbana* than in *Chromulina* sp. ($P < 0.05$; Table S3; Fig. 5g). The effect size of UVR was inhibitory in *Chromulina* sp. but strongly (>200%) stimulatory in *I. galbana* ($P < 0.05$; Table S3; Fig. 5g). Finally, the effect size of temperature × UVR was stimulatory in both species, particularly in *I. galbana* ($P < 0.05$; Table S3; Fig. 5g).

For each species and experimental condition, the difference between specific-BV and specific-PP (i.e., BV minus PP) from the results of the effect size (Fig. 5, b and e) is summarized in Figure 6. Our findings reveal that, while temperature exerted a common effect of stimulating the phagotrophic machinery with respect to photosynthesis in both species, UVR stimulated phagotrophy more in *Chromulina* sp. and the phototrophy more in *Isochrysis galbana*. Notably, the joint effect of temperature and UVR favored phototrophy machinery over phagotrophy in both cells.

DISCUSSION

This study answered the key question concerning how the metabolic response to multiple stressors can differ in protists located in different positions along the mixotrophic gradient. We found two remarkable results: the first refered to the nutritional strategy of both species, while the second refered to the magnitude and direction of the effect of global-change factors on cell metabolism and the underlying mechanisms.

First, our results indicated that *Isochrysis galbana* has a proportionally greater dependence on photosynthesis than on phagotrophy, in agreement with Cabrerizo et al. (2017), and Anderson et al. (2018). However, *Chromulina* sp. acted more autotrophically than reported by Rottberger et al. (2013) and Jones and Ilmavirta (1988). Therefore, our study revealed that *I. galbana* and *Chromulina* sp. were closer to autotrophy than to heterotrophy on the continuum of nutritional strategies established for mixotrophy by Mitra et al. (2016).

Despite that *Isochrysis galbana* exhibited a mostly autotrophic metabolism (high PP:BV values), this species displayed notable bacterivorous activity that corresponded to a higher respiratory rate and lower levels of NPQ than those shown by *Chromulina* sp.

The daily Φ_{PSII} differed between the two species, with *Chromulina* sp. showing the typical "U-shaped" curve during light-dark period, whereas *Isochrysis galbana* registered the strongest inhibition at the

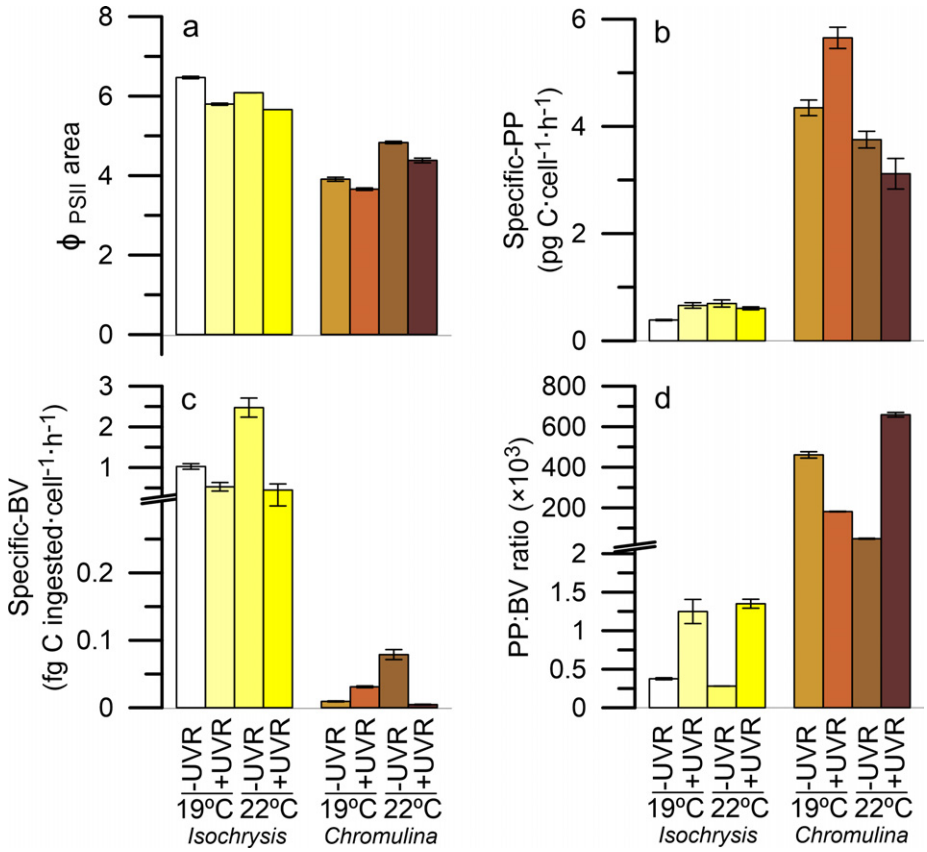

FIG. 4. Metabolic variables of *Isochrysis galbana* and *Chromulina* sp. under temperature (T) (low T [19°C] and high T [22°C]) and Light (full sunlight [+UVR] photosynthetically active radiation [−UVR]) treatments. Area under the curve for effective quantum yield (Φ_{PSII} area) (a), Specific primary production (specific-PP), (b), specific-bacterivory (specific-BV), (c) and PP:BV ratio (d). Data are expressed as mean values ± SD (n = 3). [Color figure can be viewed at wileyonlinelibrary.com]

beginning of dark period (Fig. S2 in the Supporting Information). Presumably, the low NPQ levels and excess light (exceeding the photosynthetic capacity of *I. galbana* and thus causing cumulative photodamage) gave rise to this atypical pattern of Φ_{PSII} (Aro et al. 1993, Ort 2001). Surprisingly, *Chromulina* sp. showed greater predominance of autotrophic metabolism—that is, the highest PP:BV values, concomitant with high values of Chl *a* and N cell quota related to the great development of the photosynthetic apparatus (Kolber et al. 1988) and with higher NPQ values. The latter values could indicate a stronger photoprotective mechanism due to high photosynthetic activity (Halac et al. 2014, Cabrerizo et al. 2018). Stoichiometrically, both species suffered mineral limitation by N (*Isochrysis galbana*) and P (*Chromulina* sp.), related to their marine and freshwater origin.

Thus, according to these capacities, *Isochrysis galbana* and *Chromulina* sp. are type II constitutive mixotrophs (Mitra et al. 2016) or "phytoplankton" that feed on bacteria (Stoecker et al. 2017), although with low ingestion rates ($0.06 \cdot \text{cell}^{-1} \cdot \text{h}^{-1}$ for *I. galbana* and $0.002 \cdot \text{cell}^{-1} \cdot \text{h}^{-1}$ for *Chromulina* sp.).

Second, our complex experimental approach considered the temporal extent and action scales of press (over 1 month of warming 3°C) and pulse (6 h of UVR disturbance) as a realistic way to determine the metabolic trade-off of mixotrophs against these two global-change drivers. Thus, this study revealed that, regardless of their main nutritional strategy, the two species showed a similar metabolic trade-off in response to warming (Fig. 6). Warming favored the phagotrophic over the photosynthetic machinery in both species (Fig. 6) according to our hypothesis and the studies of Wilken et al. (2012) and Chan et al. (2018). For *Isochrysis galbana*, warming also stimulated specific-PP, apparently mediated by increasing metabolic pathways (i.e., RuBisCO; Helbling et al. 2011). The results also showed a notable mismatch between Φ_{PSII} and PP, as reported by Behrenfeld et al. (1998) and Gilbert et al. (2000). That Φ_{PSII} was inhibited (as also reported by Cabrerizo et al. 2018) and specific-PP stimulated by temperature was due probably to a change in coupling between electron transfer and C fixation (Moore et al. 2003, Wagner et al. 2006, Carrillo et al. 2015). The stimulation of both types of metabolism in *I. galbana* appears to be related to

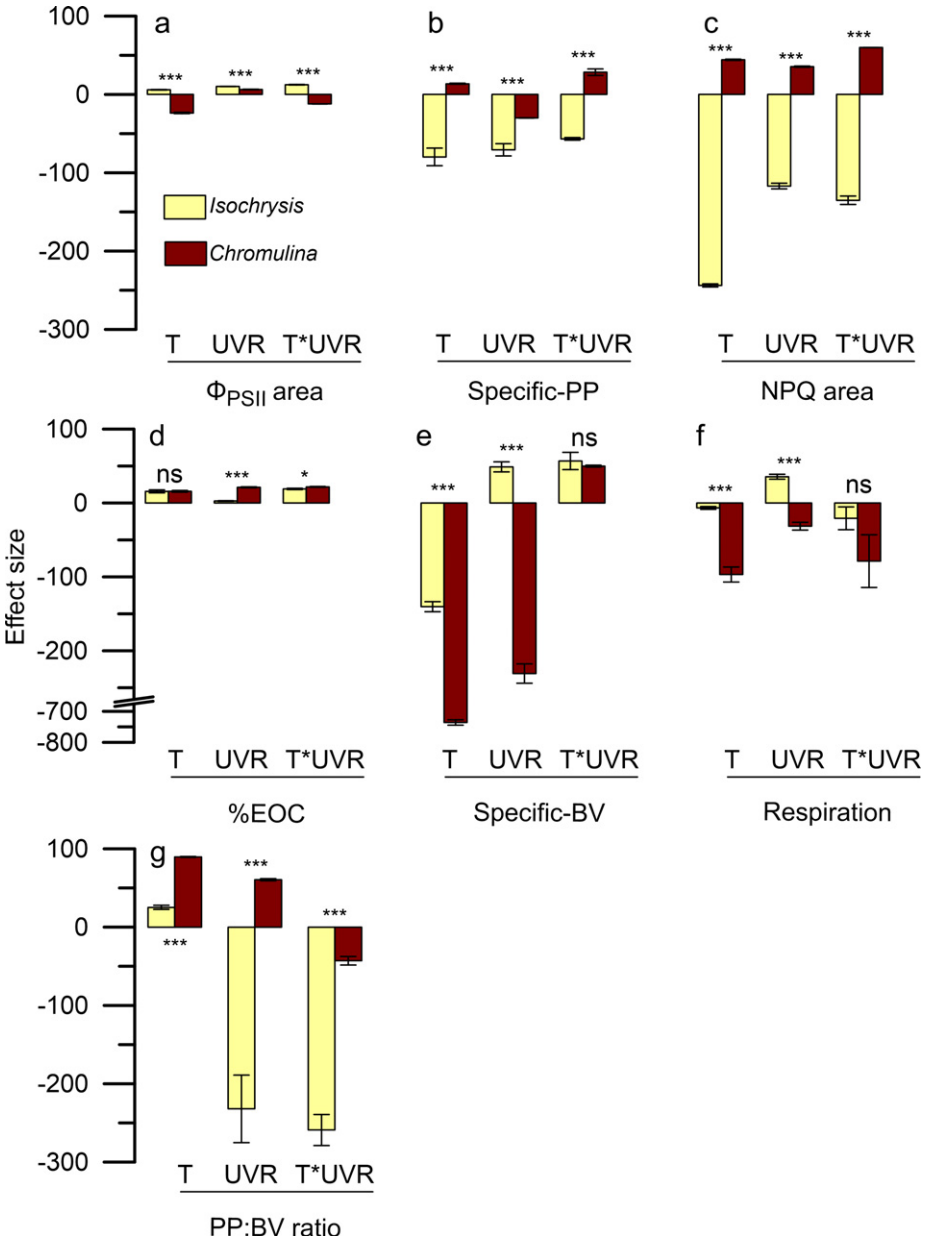

FIG. 5. Effect size of temperature (T), UVR, and temperature (T) × UVR effect for the variables area under the curve for effective quantum yield (Φ_{PSII} area), (a) Specific primary production (specific-PP), (b) area under the curve for nonphotochemical quenching (NPQ area), (c) percentage of excreted organic carbon (%EOC), (d) specific-bacterivory (specific-BV), (e) respiration (R), (f) and PP:BV ratio (g) for *Isochrysis galbana* and *Chromulina* sp. Data are expressed as mean values ± SD ($n = 3$). Asterisks show the significance value: ***$P < 0.001$; *$P < 0.05$; ns: not significant. [Color figure can be viewed at wileyonlinelibrary.com]

greater values for NPQ (Halac et al. 2014) and R (Smith et al. 2015). However, temperature as a single factor exerted a negative effect on specific-PP of *Chromulina* sp., in agreement with the results reported by Princiotta et al. (2016) for the chrysophyte *Dinobryon sociale* and by Sutton (1972) for *Chromulina chionophila*. It is plausible that high temperature and the inhibition of NPQ to quench the excess of energy might provoke an accumulation of photodamage in *Chromulina* sp. Regarding cell stoichiometry, the absence of a significant effect of warming agrees with lack of response of C:N ratio of phytoplankton community to temperature increase (Yvon-Durocher et al. 2017), although Yvon-Durocher et al. (2015) reported a higher N:P and C:P ratio under warming conditions for natural communities due to the decline of P-rich assembly machinery (ribosomes) relative to N-rich photosynthetic machinery.

The two species differed in their metabolic tradeoff in response to UVR and it was similar for temperature × UVR (Fig. 6). Contrary to our

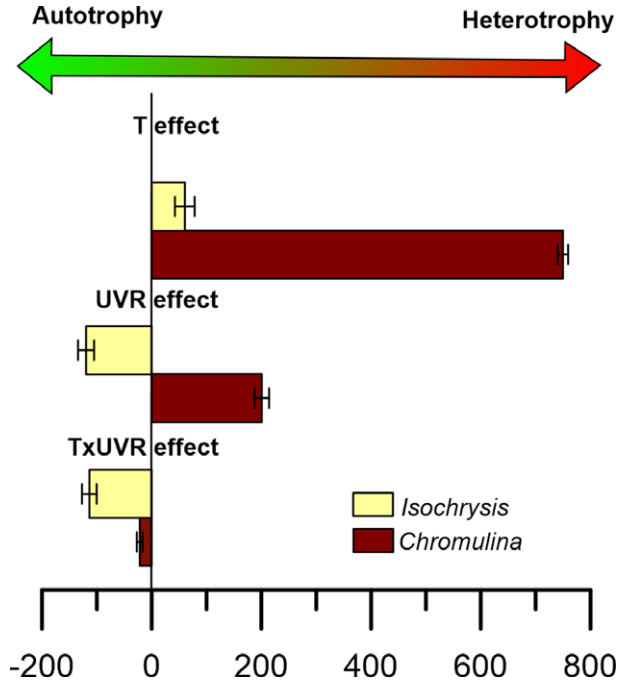

FIG. 6. Comparative of machinery stimulation of specific primary production (specific-PP) or specific-bacterivory (specific-BV) in *Isochrysis galbana* and *Chromulina* sp. calculated as the difference between specific-BV and specific-PP from the results of the effect size of each factor (temperature [T], UVR and temperature [T] × UVR). [Color figure can be viewed at wileyonlinelibrary.com]

hypothesis, UVR and temperature × UVR moved the cell metabolism of *Isochrysis galbana* toward autotrophy because of a stimulation of specific-PP and inhibition of specific-BV. The stimulation of specific-PP (also reported by Gao et al. 2007) was related to higher values of NPQ, consistent with their photoprotective function under UVR (Halac et al. 2014). The negative effect of UVR on specific-BV could be related to damage to the flagellar apparatus, leading to changes in cell morphology and motility (Sommaruga et al. 1996, Sommaruga and Buma 2000). A positive effect of temperature × UVR on BV and a negative one on the electron-transport rate of *Isochrysis galbana* has been reported by Cabrerizo et al. (2018). By contrast, single UVR stimulated mainly phagotrophy in *Chromulina* sp., whereas temperature × UVR displaced the metabolism toward phototrophy. The phagotrophic ability of chrysophytes such as *Ochromonas* sp. and *Chromulina nevadensis* has been proposed as an adaptive strategy at high UVR levels in aquatic ecosystems (Carrillo et al. 2017, González-Olalla et al. 2018). This strategy could be based on the ability to circumvent the photoinhibition of PSII using only the PSI (Wilken et al. 2014) and deriving C from bacterial consumption. However, guided by specific-PP inhibition by temperature, the interaction temperature × UVR exerted a negative effect on the *Chromulina* sp., also inhibiting the specific-BV. In some species, phagotrophy is light-dependent, indicating that this species may need to synthesize some factor(s) during photosynthesis (Caron et al. 1993, Zhang and Watanabe 2001). On this basis, *Chromulina* sp. could be considered an obligate phototroph.

In addition, cell stoichiometry was affected by UVR and temperature × UVR, both species exhibiting more balanced C:N ratios (close to 7.0) and N:P ratios (close to 16.0). Specifically, in *Isochrysis galbana* the C:N ratio rose and the N:P ratio fell, whereas in *Chromulina* sp. the nutrient ratio response was the opposite. These results contrast with others that have reported a fall in the C:N ratio in epilithic algae under UVR exposure (Tank et al. 2003) or no effect on marine phytoplankton (Carrillo et al. 2015). It bears noting that the stoichiometry after the action of the factors assayed became balanced, precluding its role as a first-order explanatory mechanism of the metabolic responses.

CONCLUSIONS

Warming and UVR induced shifts in the cell metabolism of both species from initial conditions, revealing a high metabolic trade-off (Fig. 6). This shift was consistently toward greater phagotrophy under a temperature increase, supporting our hypothesis. However, our study proved that temperature increase and UVR simultaneously affected the phototrophic and phagotrophic machinery in both mixotrophic protists, moving their metabolism toward greater autotrophy. The decrease in mixotrophy, driven by low phagotrophic activity, under temperature × UVR conditions could negatively affect the bypass of C flux through the bacteria-mixotroph link (Medina-Sánchez et al. 2004, Ptacnik et al. 2016), resulting in less efficient C flux and transfer inorganic nutrients in the aquatic food webs.

The authors are grateful to Virginia Margenet for her help in the laboratory analysis. We thank David Nesbitt for English-writing assistance. We appreciate the contribution and comments on early drafts of our manuscript by Editor Thomas Mock, Dr. Douglas Campbell and two anonymous reviewers. This study was supported by Ministerio Economía y Competitividad and Fondo Europeo de Desarrollo Regional (FEDER) (CGL2015–67682-R to P.C. and J.M.M.-S.). J.M.G.-O. was supported by the Spanish Government Fellowship "Formación de Profesorado Universitario" (FPU14/00977).

Anderson, R., Charvet, S. & Hansen, P. J. 2018. Mixotrophy in chlorophytes and haptophytes—Effect of irradiance, macronutrient, micronutrient and vitamin limitation. *Front. Microbiol.* 9:1704.

APHA. 1992. *Standard Methods for the Examination of Water and Wastewater.* American Public Health Association, Washington, DC, USA.

Aro, E. M., Virgin, I. & Andersson, B. 1993. Photoinhibition of photosystem II. Inactivation, protein damage and turnover. *Biochim. Biophys. Acta* 1143:113–34.

Behrenfeld, M. J., Prasil, O., Kolber, Z. S., Babin, M. & Falkowski, P. G. 1998. Compensatory changes in Photosystem II

electron turnover rates protect photosynthesis from photoinhibition. *Photosynth. Res.* 58:259–68.

Bell, T. B., Ahlgren, G. M. & Ahlgren, I. 1983. Estimating bacterioplankton production by measuring ^{3}H-thymidine incorporation in a eutrophic Swedish lake. *Appl. Environ. Microbiol.* 45:1709–21.

Buma, A. G. J., Boelen, P. & Jeffrey, W. 2003. UVR- induced DNA damage in aquatic organisms. *In* Helbling, E. W. & Zagarese, H. E. [Eds.] *UV Effects in Aquatic Organisms and Ecosystems. Comprehensive Series in Photochemical and Photobiological Sciences.* The Royal Society of Chemistry, Cambridge, pp. 291–327.

Cabrerizo, M. J., Carrillo, P., Villafañe, V. E. & Helbling, E. W. 2014. Current and predicted global change impacts of UVR, temperature and nutrient inputs on photosynthesis and respiration of key marine phytoplankton groups. *J. Exp. Mar. Biol. Ecol.* 461:371–80.

Cabrerizo, M. J., González-Olalla, J. M., Hinojosa-López, V. J., Peralta-Cornejo, F. J. & Carrillo, P. 2018. A shifting balance: responses of mixotrophic marine algae to cooling and warming under UVR. *New Phytol.* 221:1317–27.

Cabrerizo, M. J., Medina-Sánchez, J. M., Dorado-García, I., Villar-Argaiz, M. & Carrillo, P. 2017. Rising nutrient-pulse frequency and high UVR strengthen microbial interactions. *Sci. Rep.* 7:43615.

Caron, D. A., Sanders, R. W., Lim, E. L., Marrasé, C., Amaral, L. A., Whitney, S., Aoki, R. B. & Porte, K. G. 1993. Light-dependent phagotrophy in the freshwater mixotrophic chrysophyte *Dinobryon cylinadricum*. *Microb. Ecol.* 25:93–111.

Carrillo, P., Medina-Sánchez, J. M., Herrera, G., Durán, C., Segovia, M., Cortés, D., Salles, S., Korbee, N., Figueroa, F. L. & Mercado, J. M. 2015. Interactive effect of UVR and phosphorus on the coastal phytoplankton community of the western Mediterranean Sea: unravelling eco-physiological mechanisms. *PLoS ONE* 10:e0142987.

Carrillo, P., Medina-Sánchez, J. M. & Villar-Argaiz, M. 2002. The interaction of phytoplankton and bacteria in a high mountain lake: importance of the spectral composition of solar radiation. *Limnol. Oceanogr.* 47:1294–306.

Carrillo, P., Medina-Sánchez, J. M., Villar-Argaiz, M., Bullejos, F. J., Durán, C., Bastidas-Navarro, M., Souza, M. S., Balseiro, E. G. & Modenutti, B. E. 2017. Vulnerability of mixotrophic algae to nutrient pulses and UVR in an oligotrophic Southern and Northern Hemisphere lake. *Sci. Rep.* 7:6333.

Chan, Y. F., Chiang, K. P., Ku, Y. & Gong, G. C. 2018. Abiotic and biotic factors affecting the ingestion rates of mixotrophic nanoflagellates (Haptophyta). *Microb. Ecol.* 3:607–615.

Del Giorgio, P. A. & Cole, J. J. 1998. Bacterial growth efficiency in natural aquatic systems. *Annu. Rev. Ecol. Syst.* 29:503–41.

Flynn, K. J., Stoecker, D. K., Mitra, A., Raven, J. A., Glibert, P. M., Hansen, P. J., Granéli, E. & Burkholder, J. M. 2013. Misuse of the phytoplankton–zooplankton dichotomy: the need to assign organisms as mixotrophs within plankton functional types. *J. Plankton Res.* 35:3–11.

Gao, K., Wu, Y., Li, G., Wu, H., Villafañe, V. E. & Helbling, E. W. 2007. Solar UV radiation drives CO_2 fixation in marine phytoplankton: a double-edged sword. *Plant Physiol.* 144:54–9.

Gilbert, M., Domin, A., Becker, A. & Wilhelm, C. 2000. Estimation of primary productivity by chlorophyll *a* in vivo fluorescence in freshwater phytoplankton. *Photosynthetica* 38:111–26.

González-Olalla, J. M., Medina-Sánchez, J. M., Cabrerizo, M. J., Villar-Argaiz, M., Sánchez-Castillo, P. M. & Carrillo, P. 2017. Contrasting effect of Saharan dust and UVR on autotrophic picoplankton in nearshore versus offshore waters of Mediterranean Sea. *J. Geophys. Res-Biogeo.* 122:2085–103.

González-Olalla, J. M., Medina-Sánchez, J. M., Lozano, I. L., Villar-Argaiz, M. & Carrillo, P. 2018. Climate-driven shifts in algal-bacterial interaction of high-mountain lakes in two years spanning a decade. *Sci. Rep.* 8:10278.

Guillard, R. R. L. & Ryther, J. H. 1962. Studies of marine planktonic diatoms. I. *Cyclotella nana* Husted, and *Detonula confervacea* (Cleve) Gran. *Can. J. Microbiol.* 8:229–39.

Halac, S. R., Guendulain-García, S. D., Villafañe, V. E., Helbling, E. W. & Banaszak, A. T. 2013. Responses of tropical plankton communities from the Mexican Caribbean to solar ultraviolet radiation exposure and increased temperature. *J. Exp. Mar. Biol. Ecol.* 445:99–107.

Halac, S. R., Villafañe, V. E., Gonçalves, R. J. & Helbling, E. W. 2014. Photochemical responses of three marine phytoplankton species exposed to ultraviolet radiation and increased temperature: role of photoprotective mechanisms. *J. Photoch. Photobio. B* 141:217–27.

Halac, S. R., Villafañe, V. E. & Helbling, E. W. 2010. Temperature benefits the photosynthetic performance of the diatoms *Chaetoceros gracilis* and *Thalassiosira weissflogii* when exposed to UVR. *J. Photoch. Photobio. B.* 101:196–205.

Harris, R. M. B., Beaumont, L. J., Vance, T. R., Tozer, C. R., Remenyi, T. A., Perkins-Kirkpatrick, S. E., Mitchell, P. J. et al. 2018. Biological responses to the press and pulse of climate trends and extreme events. *Nat. Clim. Change.* 8:579–87.

Helbling, E. W., Buma, A. G., Boelen, P., van der Strate, H. J., Fiorda Giordanino, M. V. & Villafañe, V. E. 2011. Increase in RuBisCO activity and gene expression due to elevated temperature partially counteracts ultraviolet radiation–induced photoinhibition in the marine diatom *Thalassiosira weissflogii*. *Limnol. Oceanogr.* 56:1330–42.

IPCC. 2013. *Climate Change 2013: The Physical Science Basis. Contribution of Working Group I to the Fifth Assessment Report of the Intergovernmental Panel on Climate Change. In* Stocker, T. F., Qin, D., Plattner, G. K., Tignor, M., Allen, S. K., Boschung, J., Nauels, A., Xia, Y., Bex, V. & Midgley, P. M. [Eds.] Cambridge University Press, Cambridge, UK and New York, NY, 1535 pp.

Jackson, M. C., Loewen, C. J. G., Vinebrooke, R. D. & Chimimba, C. T. 2016. Net effects of multiple stressors in freshwater ecosystems: a meta-analysis. *Glob. Change Biol.* 22:180–9.

Joint, I. & Jordan, M. B. 2008. Effect of short-term exposure to UVA and UVB on potential phytoplankton production in UK coastal waters. *J. Plankton Res.* 30:199–210.

Jones, R. & Ilmavirta, V. 1988. *Flagellates in Freshwater Ecosystems. Dev. Hydrob.* Springer Netherlands, Dordrecht, 288 pp.

Kolber, Z., Zehr, J. & Falkowski, P. 1988. Effects of growth, irradiance and nitrogen limitation on photosynthetic energy conversion in photosystem II. *Plant Physiol.* 88:923–9.

Lee, S. & Fuhrman, J. A. 1987. Relationships between biovolume and biomass of naturally derived marine bacterioplankton. *Appl. Environ. Microbiol.* 53:1298–303.

Lignell, R. 1992. Problems in filtration fractionation of ^{14}C primary productivity samples. *Limnol. Oceanogr.* 37:172–8.

Maxwell, K. & Johnson, G. N. 2000. Chlorophyll fluorescence—A practical guide. *J. Exp. Bot.* 51:659–68.

Medina-Sánchez, J. M., Villar-Argaiz, M. & Carrillo, P. 2004. Neither with nor without you: a complex algal control on bacterioplankton in a high mountain lake. *Limnol. Oceanogr.* 49:1722–33.

Mitra, A., Flynn, K. J., Burkholder, J. M., Berge, T., Calbet, A., Raven, J. A., Granéli, E. et al. 2014. The role of mixotrophic protist in the biological carbon pump. *Biogeosciences* 11:995–1005.

Mitra, A., Flynn, K. J., Tillmann, U., Raven, J. A., Caron, D., Stoecker, D. K., Not, F. et al. 2016. Defining planktonic protist functional groups on mechanisms for energy and nutrient acquisition: incorporation of diverse mixotrophic strategies. *Protist* 167:106–20.

Modenutti, B. 2014. Mixotrophy in Argentina freshwaters. *Advanc. Limnol.* 65:359–74.

Montagnes, D. J. S., Morgan, G., Bissinger, J. E., Atkinson, D. & Weisse, T. 2008. Short-term temperature change may impact freshwater carbon flux: amicrobial perspective. *Glob. Change Biol.* 14:2810–22.

Moore, M. C., Suggett, D. J., Holligan, P. M., Sharples, J. & Abrahams, E. R. 2003. Physical controls on phytoplankton physiology at a shelf front: a fast repetition-rate fluorometer based field study. *Mar. Ecol. Prog. Ser.* 259:29–45.

Mühling, M., Harris, N., Belay, A. & Whitton, B. A. 2003. Reversal of helix orientation in the Cyanobacterium *Arthrospira*. *J. Phycol.* 39:360–7.

Ort, D. R. 2001. When there is too much light. *Plant Physiol.* 125:29–32.

Princiotta, S. D., Smith, B. T. & Sanders, R. W. 2016. Temperature-dependent phagotrophy and phototrophy in a mixotrophy *Chrysophyte*. *J. Phycol.* 52:432–40.

Ptacnik, R., Gomes, A., Royer, S. J., Berger, S. A., Calbet, A., Nejstgaard, J. C., Gasol, J. M. et al. 2016. A light-induced shortcut in the planktonic microbial loop. *Sci. Rep.* 6:29286.

Raven, J. A., Beardall, J., Flynn, K. J. & Maberly, S. C. 2009. Phagotrophy in the origins of photosynthesis in eukaryotes and as a complementary mode of nutrition in phototrophs: relation to Darwin's insectivorous plants. *J. Exp. Bot.* 60:3975–87.

Reusch, T. B. H. & Boyd, P. W. 2013. Experimental evolution meets marine phytoplankton. *Evolution* 67:1849–59.

Rojo, C., Herrera, G., Rodrigo, M. A., Ortíz-Llorente, M. J. & Carrillo, P. 2012. Mixotrophic phytoplankton is enhanced by UV radiation in a low altitude, P-limited Mediterranean lake. *Hydrobiologia* 698:97–110.

Rottberger, J., Gruber, A., Boenigk, J. & Kroth, P. G. 2013. Influence of nutrients and light on autotrophic, mixotrophic and heterotrophic freshwater chrysophytes. *Aquat. Microb. Ecol.* 71:179–91.

Selosse, M. A., Charpin, M. & Not, F. 2017. Mixotrophy everywhere on land and in water: the grand écart hypothesis. *Ecol. Lett.* 20:246–63.

Smith, R. T., Bangert, K., Wilkinson, S. J. & Gilmour, D. J. 2015. Synergistic carbon metabolism in a fast growing mixotrophic freshwater microalgal species *Micractinium inermum*. *Biomass Bioenerg.* 82:73–86.

Sobrino, C. & Neale, P. J. 2007. Short-term and long-term effects of temperature on photosynthesis in the diatom *Thalassiosira pseudonana* under UVR exposures. *J. Phycol.* 43:426–36.

Sommaruga, R. & Buma, A. G. J. 2000. UV-induced cell damage is species-specific among aquatic phagotrophic protists. *J. Eukaryot. Microbiol.* 47:450–5.

Sommaruga, R., Oberleiter, A. & Psenner, R. 1996. Effect of UV radiation on the bacterivory of a heterotrophic nanoflagellate. *Appl. Environ. Microbiol.* 62:4395–400.

StatSoft Inc. 2005. Electronic Statistics Textbook. Tulsa, OK: StatSoft. [on-line] WEB: http://www.statsoft.com/textbook/stathome.html.

Steemann Nielsen, E. 1952. The use of radio-active carbon (C14) for measuring organic production in the sea. *J. Conseil* 18:117–40.

Stoecker, D. K., Hansen, P. J., Caron, D. A. & Mitra, A. 2017. Mixotrophy in the marine plankton. *Annu. Rev. Mar. Sci.* 9:311–35.

Sutton, E. A. 1972. The physiology and life histories of selected Chrysophytes of the Pacific Northwest. PhD thesis, Oregon State University, Corvalis, Oregon, USA, 107 pp.

Takabayashi, M., Lew, K., Johnson, A., Marchi, A. L., Dugdale, R. & Wilkerson, F. P. 2006. The effect of nutrient availability and temperature on chain length of the diatom, *Skeletonema costatum*. *J. Plankton Res.* 28:831–40.

Takahashi, S., Yoshioka-Nishimura, M., Nanba, D. & Badger, M. R. 2013. Thermal acclimation of the symbiotic alga *Symbiodinium* spp. alleviates photobleaching under heat stress. *Plant Physiol.* 161:477–85.

Tank, S. E., Schindler, D. W. & Arts, M. T. 2003. Direct and indirect effects of UV radiation on benthic communities: epilithic food quality and invertebrate growth in four montane lakes. *Oikos* 103:651–67.

Tsai, S. F., Lin, F. W., Chan, Y. F. & Chiang, K. P. 2016. Vertical distribution of pigmented and non-pigmented nanoflagellates in the East China Sea. *Cont. Shelf Res.* 125:107–13.

Unrein, F., Massana, R., Alonso-Saez, L. & Gasol, J. M. 2007. Significant year-round effect of small mixotrophic flagellates on bacterioplankton in an oligotrophic coastal system. *Limnol. Oceanogr.* 52:456–69.

Verity, P. G. 1981. Effects of temperature, irradiance, and daylength on the marine diatom *Leptocylindrus danicus* cleve. I. Photosynthesis and cellular composition. *J. Exp. Mar. Biol. Ecol.* 55:79–91.

Villafañe, V. E., Banaszak, A. T., Guendulain-García, S. D., Strauch, S. M., Halac, S. R. & Helbling, E. W. 2013. Influence of seasonal variables associated with climate change on photochemical diurnal cycles of marine phytoplankton from Patagonia (Argentina). *Limnol. Oceanogr.* 58:203–14.

Villafañe, V. E., Sundbäck, K., Figueroa, F. L. & Helbling, E. W. 2003. Photosynthesis in the aquatic environment as affected by UVR. *In* Helbling, E. W. & Zagarese, H. E. [Eds.] *UV Effects in Aquatic Organisms and Ecosystems, Comprehensive Series in Photochemistry & Photobiology*. The Royal Society of Chemistry, Cambridge, pp. 357–97.

Villar-Argaiz, M., Medina-Sánchez, J. M., Biddanda, B. A. & Carrillo, P. 2018. Predominant non-additive effects of multiple stressors on autotroph C:N: P ratios propagate in freshwater and marine food webs. *Front. Microbiol.* 9:69.

Wagner, H., Jakob, T. & Wilhelm, C. 2006. Balancing the energy flow from captured light to biomass under fluctuating light conditions. *New Phytol.* 169:95–108.

Ward, B. A. & Follows, M. J. 2016. Marine mixotrophy increases trophic transfer efficiency, mean organism size, and vertical carbon flux. *Proc. Natl. Acad. Sci. USA* 113:2958–63.

Wilken, S., Huisman, J., Naus-Wiezer, S. & Van Donk, E. 2012. Mixotrophic organisms become more heterotrophic with rising temperature. *Ecol. Lett.* 16:225–33.

Wilken, S., Schuurmans, J. M. & Matthijs, H. C. P. 2014. Do mixotrophs grow as photoheterotrophs? Photophysiological acclimation of the chrysophytes *Ochromonas danica* after feeding. *New Phytol.* 204:882–9.

Yvon-Durocher, G., Dossena, M., Trimmer, M., Woodward, G. & Allen, A. P. 2015. Temperature and the biogeography of algal stoichiometry. *Glob. Ecol. Biogeogr.* 24:562–70.

Yvon-Durocher, G., Schaum, C. E. & Trimmer, M. 2017. The temperature dependence of phytoplankton stoichiometry: investigating the roles of species sorting and local adaptation. *Front. Microbiol.* 8:2003.

Zhang, X. & Watanabe, M. M. 2001. Grazing and growth of the mixotrophic Chrysomonad *Poterioochromonas malhamensis* (Chrysophyceae) feeding on algae. *J. Phycol.* 37:738–43.

Zubkov, M. V. & Tarran, G. A. 2008. High bacterivory by the smallest phytoplankton in the North Atlantic Ocean. *Nature* 455:224–6.

Supporting Information

Additional Supporting Information may be found in the online version of this article at the publisher's web site:

Figure S1. Metabolic and physiologic variables of *Isochrysis galbana* and *Chromulina* sp. under Temperature (T) (low T [19°C] and high T [22°C]) and Light (full sunlight [+UVR] photosynthetically active radiation [−UVR]) treatments. Respiration (R), (a), percentage of excreted organic carbon (%EOC), (b) and area under the curve for nonphotochemical quenching (NPQ area), (c) for *Isochrysis galbana* and *Chromulina* sp. Data are expressed as mean values ± SD (n = 3).

Figure S2. Photobiological variables of *Isochrysis galbana* and *Chromulina* sp. under Temperature (T) (low T [19°C] and high T [22°C]) and Light (full sunlight [+UVR] photosynthetically active

radiation [−UVR]) treatments. Effective quantum yield (Φ_{PSII}) (a, b) and nonphotochemical quantum yield (NPQ), (c,d) values for *I. galbana* (left panel) and *Chromulina* sp. (right panel). Horizontal white and shaded areas on "X axis, time" represent the light and dark exposure period, respectively, throughout the experiment.

Table S1. Results of the *t*-tests for independent samples to analyze the differences between species for each response variable (cell-specific Chl *a*, C cell quota, N cell quota and P cell quota, C:N and N:P ratios, area under the curve for photochemical quantum yield area [Φ_{PSII} area], specific primary production [sPP], specific-bacterivory [sBV], PP:BV ratio, area under the curve for nonphotochemical quenching area [NPQ area], percentage of excreted organic carbon [%EOC], and respiration [R]), under identical experimental conditions.

Table S2. Results of the two-way split-plot analysis of variance of Temperature (T) and UVR effects on cell-specific Chl *a*, C cell quota, N cell quota and P cell quota, C:N and N:P ratios. Numbers in bold indicate significant effect.

Table S3. Results of the *t*-test for independent samples to analyze the differences between species on the variables (cell-specific Chl *a*, C cell quota, N cell quota and P cell quota, C:N and N:P ratios, area under the curve for photochemical quantum yield area [Φ_{PSII} area], specific primary production [sPP], specific-bacterivory [sBV], PP:BV ratio, area under the curve for nonphotochemical quenching area [NPQ area], percentage of excreted organic carbon [%EOC], and respiration [R]), for the effect size of T, UVR, and T × UVR.

Table S4. Results of the two-way split-plot analysis of variance of Temperature (T) and UVR effects on area under the curve for photochemical quantum yield area (Φ_{PSII} area), specific primary production (sPP), specific-bacterivory (sBV), PP:BV ratio, area under the curve for nonphotochemical quenching area (NPQ area), percentage of excreted organic carbon (%EOC), and respiration (R). Numbers in bold indicate significant effect.